

Potentialiation of the glutamatergic synaptic input to rat locus coeruleus neurons by P2X7 receptors

Roghayeh Khakpay · Daniel Polster · Laszlo Köles ·
Andrey Skorinkin · Bela Szabo · Kerstin Wirkner ·
Peter Illes

Received: 12 March 2010 / Accepted: 14 July 2010 / Published online: 30 July 2010
© Springer Science+Business Media B.V. 2010

Abstract Locus coeruleus (LC) neurons in a rat brain slice preparation were superfused with a Mg^{2+} -free and bicuculline-containing external medium. Under these conditions, glutamatergic spontaneous excitatory postsynaptic currents (sEPSCs) were recorded by means of the whole-cell patch-clamp method. ATP, as well as its structural analogue 2-methylthio ATP (2-MeSATP), both caused transient inward currents, which were outlasted by an increase in the frequency but not the amplitude of the sEPSCs. PPADS, but not suramin or reactive blue 2 counteracted both effects of 2-MeSATP. By contrast, α,β -methylene ATP (α,β -meATP), UTP and BzATP did not cause an inward current response. Of these latter agonists, only BzATP slightly facilitated the sEPSC amplitude and strongly potentiated its frequency. PPADS and Brilliant Blue G, as well as

fluorocitric acid and aminoadipic acid prevented the activity of BzATP. Furthermore, BzATP caused a similar facilitation of the miniature (m)EPSC (recorded in the presence of tetrodotoxin) and sEPSC frequencies (recorded in its absence). Eventually, capsaicin augmented the frequency of the sEPSCs in a capsazepine-, but not PPADS-antagonizable, manner. In conclusion, the stimulation of astrocytic P2X7 receptors appears to lead to the outflow of a signalling molecule, which presynaptically increases the spontaneous release of glutamate onto LC neurons from their afferent fibre tracts. It is suggested, that the two algogenic compounds ATP and capsaicin utilise separate receptor systems to potentiate the release of glutamate and in consequence to increase the excitability of LC neurons.

Keywords Adenosine 5'-triphosphate · P2X7 receptors · Presynaptic modulation · Spontaneous excitatory postsynaptic currents · Miniature excitatory postsynaptic currents · Locus coeruleus

Roghayeh Khakpay and Daniel Polster equally contributed to this work.

R. Khakpay · D. Polster · L. Köles · K. Wirkner · P. Illes (✉)
Rudolf-Boehm-Institute of Pharmacology and Toxicology,
University of Leipzig,
Haertelstrasse 16-18,
04107 Leipzig, Germany
e-mail: Peter.Illes@medizin.uni-leipzig.de

L. Köles
Department of Pharmacology and Pharmacotherapy,
Semmelweis University,
1089 Budapest, Hungary

A. Skorinkin
Institute of Physics, Kazan State University,
420008 Kazan, Russia

B. Szabo
Department of Experimental and Clinical
Pharmacology and Toxicology, University of Freiburg,
79104 Freiburg im Breisgau, Germany

Introduction

The sensation of pain is subject to descending control from higher centres of the CNS, such as the mid-pontine nucleus locus coeruleus (LC), containing a dense population of noradrenergic cell bodies [1]. The LC obtains prominent glutamatergic and GABAergic inputs from the nucleus paragigantocellularis lateralis in the rostral ventral medulla, which is implicated in several functions including pain and analgesia [2]. LC neurons are endowed with somatic nucleotide receptors of the P2X (ligand-gated cationic channels) and P2Y (G protein-coupled receptors) types, mediating rapid and slow depolarizations, respectively [3, 4]. These effects are opposite to those induced by the

activation of hyperpolarization and analgesia-mediating somatic α_2 and opioid μ receptors [5].

Focal electrical stimulation evokes, in LC brain slices, biphasic synaptic potentials, consisting of early depolarizing (DSP) and late hyperpolarizing (IPSP) components. It has been shown that a large fraction of the DSP is due to the release of glutamate, from afferent fibres, predominantly onto non-NMDA receptors and GABA onto GABA_A receptors [6, 7]. The IPSP is caused by the release of noradrenaline onto α_2 adrenoceptors from recurrent axon collaterals of the LC neurons themselves [8]. However, a residual fraction of the DSP is evoked by ATP, which may be a co-transmitter of noradrenaline and/or glutamate [9, 10].

P2X7 receptors differ in many respects from the other subtypes of this family (P2X1-6). Whereas the short-time stimulation of P2X7 leads to the expected activation of cationic currents, upon repeated or prolonged ATP application the opening of a large membrane pore can be detected [11]. The main distinguishing pharmacological properties of this receptor are the following: (1) a low-agonist potency of ATP, considerably surmounted by that of its structural analogue dibenzoyl-ATP (BzATP), (2) inhibition by various divalent cations including Ca^{2+} and Mg^{2+} , and (3) blockade of the ATP effect by a range of selective antagonists, such as Brilliant Blue G [12, 13].

In view of the great significance of peripheral P2X7 receptors in pain and inflammation [14, 15], we set out to investigate the possible role of this receptor in the central modulation of pain via the LC. We recorded in LC slices excitatory synaptic currents (sEPSCs) due to the spontaneous release of glutamate from afferent fibres and searched for the presence of P2X7 receptors facilitating the glutamatergic input. It appeared that such receptors are located at neighbouring astrocytes, releasing a further excitatory molecule, which in turn acted at the terminals of the glutamatergic afferents. Capsaicin-, pH- and heat-sensitive transient receptor potential vanilloid 1 (TRPV1) [16] receptors at LC neurons exerted an effect similar to that of P2X7 receptor agonists, but operated via independent pathways.

Methods

Brain slice preparation

Mid-pontine slices of the rat brain (150–200 μm thick) containing the caudal part of the LC were prepared from 12- to 15-day-old Wistar rats as described previously [17]. Subsequently, a single slice was fully submerged in a recording chamber (300–400 μl volume) and was superfused with oxygenated Mg^{2+} -free artificial cerebrospinal

fluid (ACSF, in mM: NaCl 126, KCl 2.5, NaH_2PO_4 1.2, CaCl_2 2.4, NaHCO_3 25, glucose 11; pH 7.4) at 3 ml/min and 22–24°C. Ascorbic acid (0.3 mM) and EDTA (0.03 mM) were present in order to prevent the oxidation of noradrenaline. In a few experiments, a MgCl_2 (1.3 mM)-containing ACSF was utilised, without any osmotic compensation. Only one brain slice was used for electrophysiological recording from each animal.

Identification of locus coeruleus neurons and patch-clamp recording

The LC was identified at the ventrolateral border of the fourth ventricle. Cells were visualised with an upright interference contrast microscope and a $\times 40$ water immersion objective (Axioscope FS, Carl Zeiss, Oberkochen, Germany). The microscope was connected to a video camera sensitive to infrared light (Newvicon C 2400-07-C; Hamamatsu, Herrsching, Germany). Patch-pipettes (tip resistance, 5–7 $\text{M}\Omega$) were prepared by a puller (Flaming-Brown P97; Sutter, Novato, CA, USA) from borosilicate capillaries and were filled with intracellular solution consisting of (in mM: potassium gluconate 140, NaCl 10, MgCl_2 3, HEPES 10, EGTA 11; pH 7.3 adjusted with KOH). The liquid junction potential (V_{LJ}) between the bath- and pipette-solution at 22°C was calculated according to Barry [18] and was found to be 14.3 mV.

Membrane currents were recorded by means of a patch-clamp amplifier (Axopatch 200B; Molecular Devices, Sunnyvale, CA, USA). Compensation of capacitance (C_m) and series resistance (R_s) was achieved with the inbuilt circuitry of the amplifier. Series resistance was compensated by 40–70% and did not change appreciably from the beginning to the end of the experiments, indicating stable recording conditions. Currents were filtered at 5–10 kHz with the inbuilt lowpass filter of the patch-clamp amplifier. Data were then sampled at 10 kHz and stored on-line with a PC using the pClamp 10.0/Clampex 10.0 software package (Molecular Devices) that was also used for data analysis.

Neurons were voltage-clamped at a holding potential of -80 mV and membrane potential values were corrected by the liquid junction potential (V_{LJ}). Noradrenaline was applied for 90 s at the beginning of each experiment in order of identifying the cells by the prominent outward current responses.

Spontaneous and miniature excitatory postsynaptic currents (sEPSCs, mEPSCs), and application of drugs

sEPSCs were recorded at the holding potential of -80 mV. Recording of mEPSCs was performed in the presence of tetrodotoxin (TTX; 0.5 μM). The postsynaptic currents

were analysed by means of the pClamp 10.0 software package, by detecting amplitudes exceeding the threshold set just above the baseline noise of the recording.

Drugs supposed to interfere with synaptic currents were applied by using three-way taps to replace the superfusion medium with another one of a modified composition. At a flow rate of 3 ml/min about 30 s were required until the drug reached the bath. Bicuculline (10 μM) was routinely added to the ACSF, at least 15 min before starting the experiment, in order to inhibit GABA_A receptor-mediated spontaneous inhibitory postsynaptic currents. When needed, P2 receptor antagonists were also superfused together with bicuculline, and were present throughout. The application periods of all P2 receptor agonists were 10 min. Average values of amplitude and frequency of sEPSCs and mEPSCs were calculated between the third and fifth minute of the control period (lasting 5 min in total), between the eighth and tenth minute of the superfusion of P2 receptor agonists, and between the eighth and tenth min of agonist washout (both lasting for 10 min in total). In some cases, percentage changes were calculated in comparison with the control period. A few brain slices were incubated for 2 h in a fluorocitric acid (FCA; 100 μM)- or amino adipic acid (AAA; 100 μM)-containing medium, before starting superfusion in the recording chamber; control measurements of the BzATP effect were made on brain slices incubated for a comparable time in drug-free ACSF.

The onset ($\tau_{\text{on}(10-90\%)}$) and offset (τ_{off}) time constants of the sEPSCs were calculated from the individual recordings by utilising an inbuilt function of the pClamp 10.0 software. The decay phases of the sEPSCs were fitted according to an exponential equation of the same software.

Drugs

The following drugs and chemicals were used: 2-methylthioadenosine triphosphate tetrasodium salt (2-MeSATP), α,β -methyleneadenosine 5'-triphosphate trisodium salt (α,β -meATP), D-2-amino adipic acid, D-(−)-2-amino-5-phosphonopentanoic acid (AP5), (−)-bicuculline methiodide, 6-cyano-7-nitroquinoxaline-2,3-dione (CNQX), suramin hexasodium salt (Tocris); adenosine 5'-triphosphate tetrasodium salt (ATP), 2'(3')-O-(4-benzoylbenzoyl)adenosine 5'-triphosphate triethylammonium salt (BzATP), DL-fluorocitric acid barium salt, L-(−)-norepinephrine (+)-bitartrate salt monohydrate, pyridoxal phosphate-6-azo(benzene-2,4-disulfonic acid) tetrasodium salt hydrate (PPADS), reactive blue 2 (Sigma-Aldrich); capsaicin, capsazepine, uridine-5'-triphosphate trisodium salt (UTP) (Calbiochem)

Stock solutions (10–100 mM) of drugs were prepared with distilled water or dimethylsulphoxide, as appropriate.

Aliquots were stored at -20°C . Further dilutions were made daily with ACSF. Equivalent quantities of the solvent had no effect.

Statistics

Results are expressed as mean \pm S.E.M. on n individual trial. Differences between means or between a mean value and zero were tested for significance by the Kruskal–Wallis ANOVA on ranks followed by the Holm–Sidak or Tukey multiple comparison procedure (SigmaStat, version 3.5; Jandel Scientific, Erkrath, Germany). Cumulative probability plots of sEPSCs/mEPSCs were constructed for inter-event intervals and compared by the Kolmogorov–Smirnov test. A probability level of 0.05 or less was considered to be statistically significant.

Results

Slice preparations were used to record membrane currents from LC neurons. In the standard Mg^{2+} -free and bicuculline (10 μM)-containing ACSF (holding potential, -80 mV), neither the amplitude (24.9 ± 1.2 pA) nor the frequency (1.8 ± 0.4 Hz) of sEPSCs changed from their control value after 18 min of superfusion with normal ACSF (26.0 ± 1.5 pA and 1.6 ± 0.3 Hz, respectively, $n=8$ each, $P>0.05$). However, the blockade of NMDA and non-NMDA receptors by AP5 (50 μM) plus CNQX (10 μM) markedly and time-dependently depressed the pre-drug amplitude and frequency of sEPSCs (Fig. 1A,B). The inhibition of sEPSC frequency was complete after 15 min of antagonist superfusion, confirming that the spontaneous synaptic currents are due to the release of glutamate.

Effects of P2 receptor agonists on sEPSCs and their interaction with P2 receptor antagonists

2-Methylthio ATP (2-MeSATP) is a structural analogue of ATP which prefers P2X over P2Y receptors, and activates all P2X receptor-types except P2X7 at the low micromolar range (10–100 μM) [19, 20]. However, the concentration (300 μM) of 2-MeSATP used in the present study should be high enough to stimulate the whole family of P2X receptors, including P2X7. 2-MeSATP caused an inward current (34.9 ± 2.2 pA, $n=7$, $P<0.05$), rapidly declining in spite of its continuous presence in the bath. Moreover, this agonist increased the frequency, but not the amplitude of sEPSCs (Fig. 2A,B). In order to quantify this effect, we calculated the amplitude and frequency of sEPSCs both during the inward current response, and after its decline to baseline, immediately before agonist washout (Fig. 2Ba,b). Although the facilitatory effect of 2-MeSATP on the sEPSC

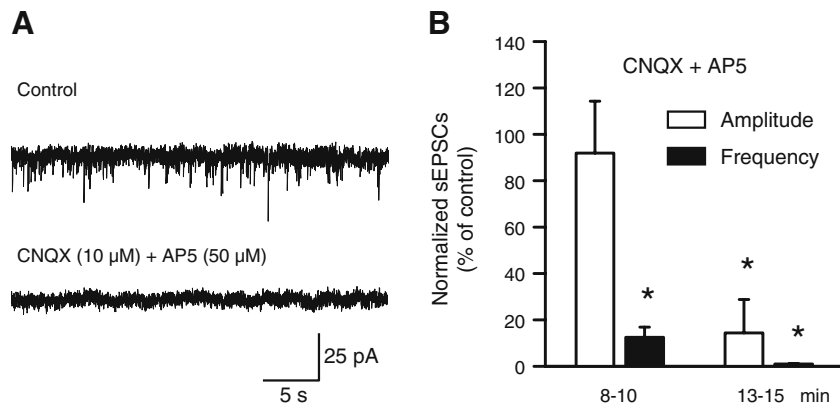


Fig. 1 Effects of AP5 and CNQX on the amplitude and frequency of sEPSCs in rat LC neurons. The holding potential in this and all following experiments was -80 mV. *A* Representative recording of sEPSCs and their abolition by a combination of the NMDA- and non-NMDA receptor antagonists AP5 ($50 \mu\text{M}$) and CNQX ($10 \mu\text{M}$),

respectively. *B* Percentage change by these antagonists of the normalised sEPSC amplitude and frequency, expressed as mean \pm S.E.M. values ($n=4$). * $P<0.05$; statistically significant differences from the control data, 8–10 and 13–15 min after drug application

frequency was more pronounced early after drug application, it persisted during the presence of the agonist for 10 min, and was completely reversible on washout. We intended to avoid a possible interference of the inward current with the increase of sEPSC frequency, and therefore evaluated all drug effects, including those of 2-MeSATP, between the 8th and 10th min after starting application. The dissociation between effects on the holding current and sEPSC frequency suggest that there are separate pre- and postsynaptic sites of action stimulated by 2-MeSATP.

In the following experiments, we investigated the interaction of 2-MeSATP with a range of non-selective P2 receptor antagonists. PPADS ($30 \mu\text{M}$) alone failed to alter

both the amplitude (control, 12.2 ± 0.6 pA; PPADS, 12.0 ± 0.5 pA; washout, 11.8 ± 0.5 pA; $P>0.05$) and frequency (control, 2.2 ± 0.5 Hz; PPADS, 2.2 ± 0.6 Hz; washout, 1.9 ± 0.5 Hz; $P>0.05$) of the sEPSCs ($n=11$ each). However, it depressed the 2-MeSATP-induced inward current (22.8 ± 3.4 pA, $n=6$, $P<0.05$; see above for control value), and abolished the enhancement of the sEPSC frequency caused by this agonist (Fig. 3Aa,Bb). In contrast, reactive blue 2 ($100 \mu\text{M}$) and suramin ($30 \mu\text{M}$) failed to alter both the inward current (40.2 ± 3.2 pA, $n=5$ and 33.2 ± 9.8 pA, $n=4$, respectively; $P>0.05$ each) and the sEPSC frequency increase (Fig. 3Ab,Bb) caused by 2-MeSATP. According to our expectations, none of the antagonists changed the sEPSC amplitudes (Fig. 3Ba).

Fig. 2 Facilitation by 2-MeSATP of the sEPSC frequency, but not amplitude in rat LC neurons. *Aa* Representative recordings of sEPSCs before (*Ab*, left panel) and 8–10 min after (*Bb*, right panel) starting superfusion with 2-MeSATP ($300 \mu\text{M}$). Note the different time-scales of recording in *Aa* and *Ab* as well as the transient inward current induced by 2-MeSATP in *Aa*. Change of the absolute amplitude (*Ba*) and frequency (*Bb*) of the sEPSCs before, during and after the application of 2-MeSATP (mean \pm S.E.M. of seven experiments). The time-period elapsing from the beginning of superfusion with 2-MeSATP is indicated. # $P<0.05$; statistically significant difference from the control value

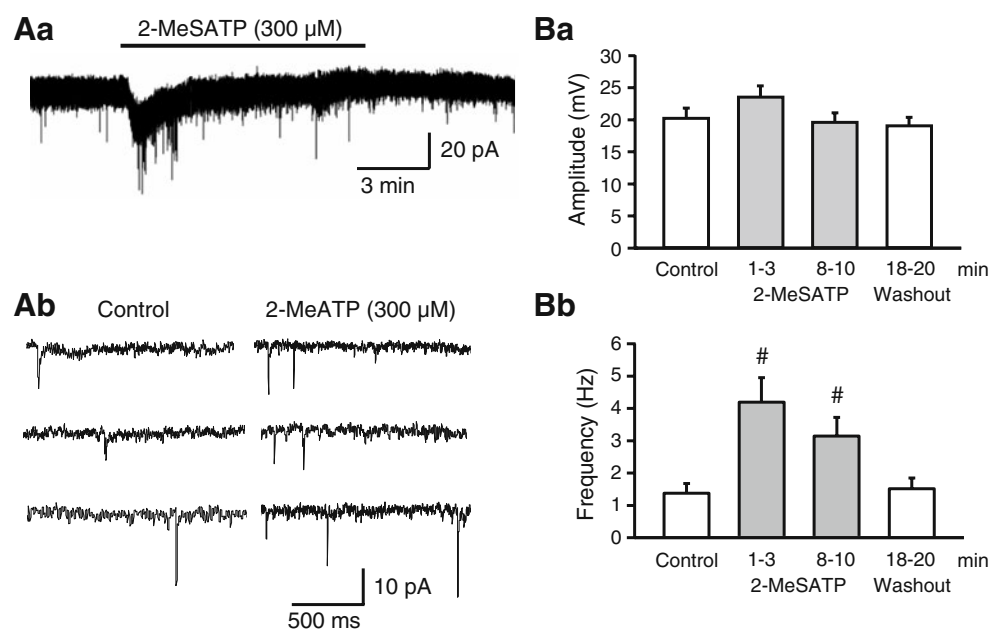
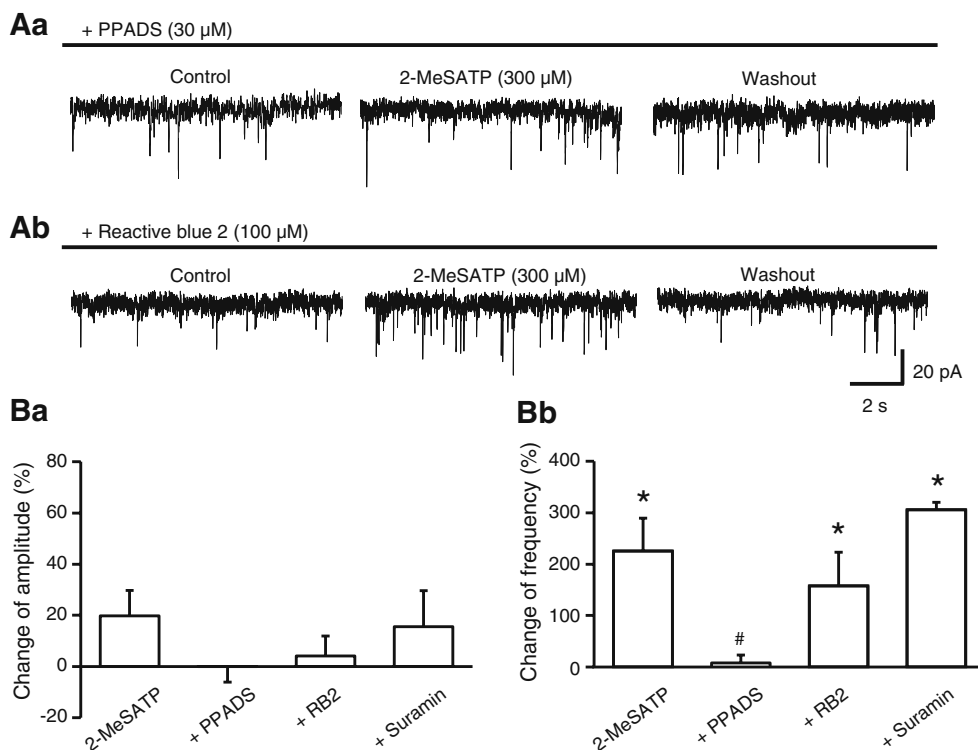


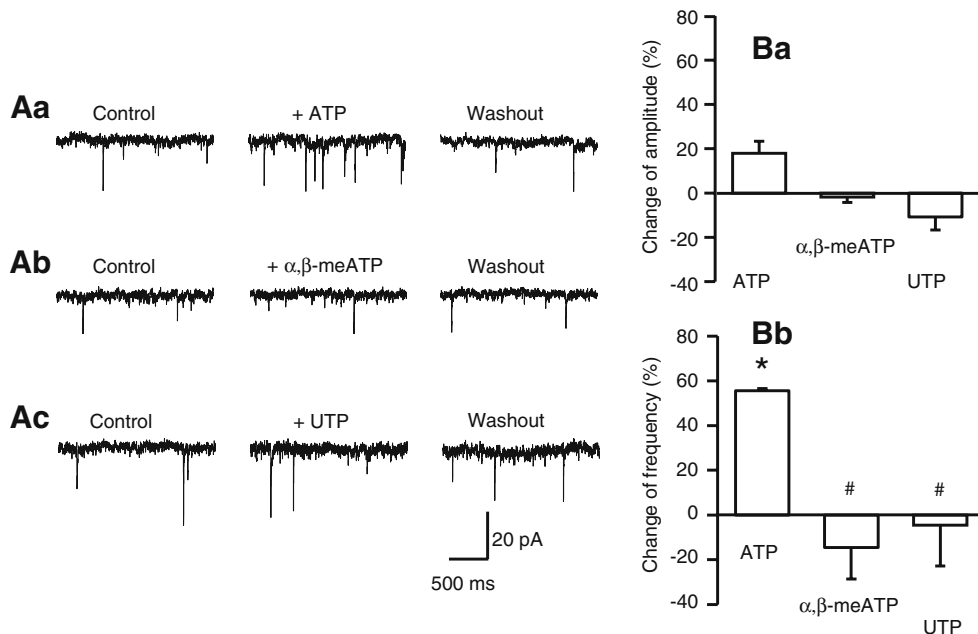
Fig. 3 Antagonism by PPADS of the 2-MeSATP-induced change in frequency of sEPSCs in rat LC neurons. *Aa* Representative recording of sEPSCs and blockade of the 2-MeSATP (300 μ M)-induced frequency potentiation by PPADS (30 μ M). *Ab* Representative recording of sEPSCs and no change of the 2-MeSATP (300 μ M)-induced frequency potentiation by reactive blue 2 (100 μ M). Percentage 2-MeSATP-induced changes of the amplitude (*Ba*) and frequency (*Bb*) of sEPSCs in the presence of PPADS, reactive blue 2 (RB2) and suramin, or their absence, 8–10 min after agonist application. Mean \pm S.E. M. of four to seven experiments. * P <0.05; statistically significant differences from zero. # P <0.05; statistically significant differences from the effect of 2-MeSATP alone



Then, in order to classify the P2 receptor-type involved, further P2 receptor agonists were tested on the LC. The endogenous non-selective P2 receptor agonist ATP (300 μ M; 60.2 ± 8.7 pA, $n=4$), but not the P2X1,3 preferential α,β -methylene ATP (α,β -meATP) (100 μ M; 8.3 ± 5.6 pA, $n=3$; $P>0.05$ each), and the P2Y2,4 preferential UTP (100 μ M; 6.2 ± 4.6 pA, $n=5$, $P>0.05$) produced an inward current. Whereas ATP facilitated the frequency

of sEPSCs, α,β -meATP and UTP (100 μ M) were without effect (Fig. 4Aa–c,Bb). None of these agonists influenced the amplitude of sEPSCs either (Fig. 4Ba). It is noteworthy that both PPADS (4.8 ± 1.8 pA, $n=4$) and suramin (14.7 ± 9.2 pA, $n=4$; $P<0.05$ each) antagonised the ATP-induced inward current. The changes of the sEPSC amplitude and frequency were not evaluated in these latter experiments.

Fig. 4 Facilitation by ATP and no effect by α,β -meATP and UTP of the sEPSC frequency in rat LC neurons. Representative recordings of the increase of the sEPSC frequency by ATP (300 μ M; *Aa*), but not α,β -meATP (100 μ M; *Ab*) and UTP (100 μ M; *Ac*). Percentage agonist-induced changes of the amplitude (*Ba*) and frequency (*Bb*) of sEPSCs, 8–10 min after agonist application. Mean \pm S.E. M. of three to five experiments. * P <0.05; statistically significant differences from zero. # P <0.05; statistically significant differences from the effect of ATP alone



Effect of BzATP on sEPSCs/mEPSCs and its interaction with P2X7 receptor antagonists as well as selective toxins of the astrocytic metabolism

BzATP (300 μM), with preference for P2X_{1,7} receptors, failed to alter the holding current of LC neurons (Fig. 5A; $n=7$). Figure 5Ca, b shows plots of the number of events against the amplitude and inter-event interval in a particular cell. When the amplitude distributions of sEPSCs were compared, a slight rightward shift was observed between the distribution obtained under control conditions and that obtained in the presence of BzATP (Fig. 5Ca). The corresponding moderate increase in the mean sEPSC amplitude is documented in Fig. 5Da. The time-course of the individual sEPSCs remained unchanged in the presence of BzATP, as indicated by the $\tau_{\text{on}(10-90\%)}$ (control, 1.33 ± 0.15 ms; BzATP, 1.44 ± 0.23 ms; $n=7$; $P>0.05$) and τ_{off} values (control, 7.16 ± 2.16 ; BzATP, 7.26 ± 1.96 ; $n=7$; $P>0.05$) (Fig. 5B). Conversely, BzATP produced a marked shift towards the right in the inter-event interval distribution

reflecting an increase of the sEPSC frequency (Fig. 5Cb, Db). The plot of the cumulative probability against the inter-event interval was accordingly displaced to the left by BzATP (Fig. 5Cb, inset). All effects were completely reversible on washing out the agonist.

Both the change in the amplitude and frequency of sEPSCs by BzATP was prevented by PPADS (30 μM), confirming the involvement of P2 receptors (Fig. 6Ba,b). Further, the sEPSC frequency increase was abolished by the selective P2X₇ receptor antagonist Brilliant Blue G (BBG; 1 μM), although the corresponding facilitation of sEPSC amplitude was left unaltered by BBG (Fig. 6Aa,Ba,b). In accordance with the finding that P2X₇ receptor-mediated effects are blocked by divalent cations, BzATP was no longer active in a Mg^{2+} -containing ACSF solution (Fig. 6Ba,b). The much larger percentage increase of the sEPSC frequency caused by BzATP (300 μM) than that produced by ATP (300 μM) itself (Figs. 4Bb and 5Db; $170.3 \pm 29.0\%$, $n=7$ vs. $54.6 \pm 1.3\%$, $n=4$, $P<0.05$) also supports the involvement of P2X₇ receptors. Eventually,

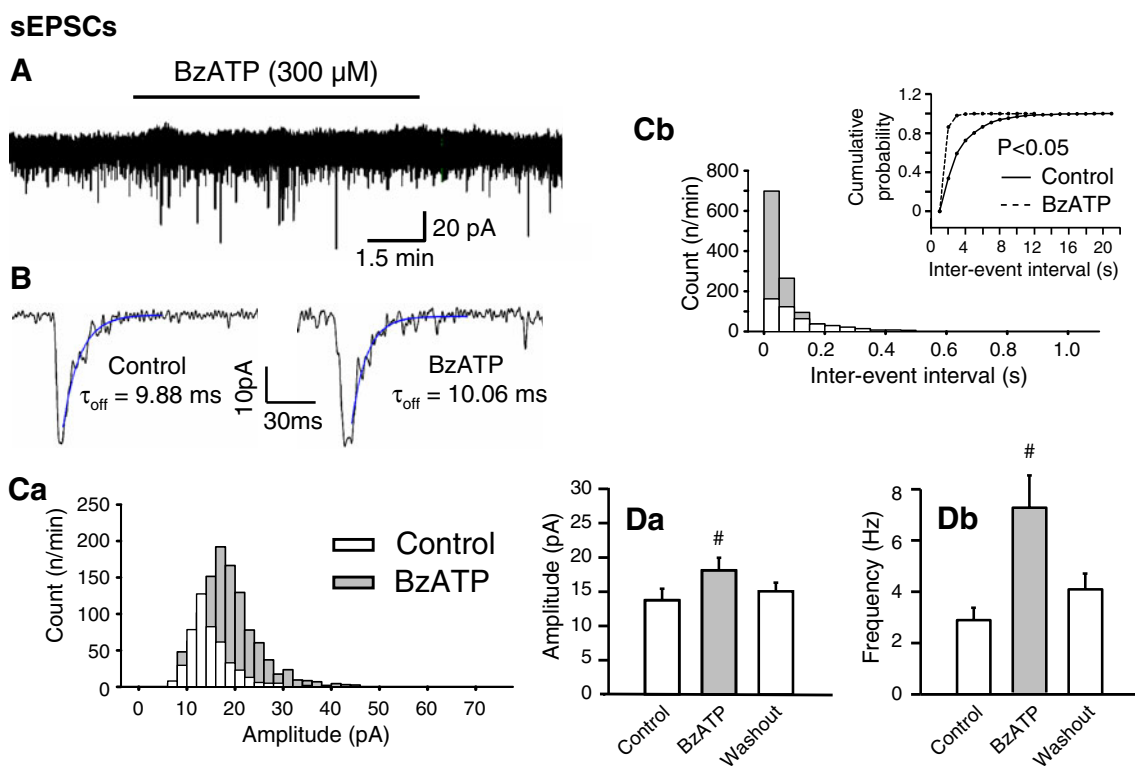


Fig. 5 Effects of BzATP on the amplitude, frequency and time-course of sEPSCs in rat LC neurons. *A* Representative recording of sEPSCs before, during and after a 10-min superfusion with BzATP (300 μM). Note the stability of the holding current in spite of the presence of BzATP. *B* Representative recordings of two sEPSCs of similar amplitude under control conditions (*left panel*) and in the presence of BzATP (*right panel*). The decay phases of the amplitudes were fitted according to a monoexponential function to calculate the offset time constants (τ_{off}). There was no change of the offset time-constant 8–10 min after the application of BzATP, when compared with the

control values (for the mean onset and offset time constants see the “Results” section). Mean \pm S.E.M. of seven experiments. *C* Plot of the number of events against the amplitude (*Ca*) and inter-event interval (*Cb*) in the cell shown in *A* and *B*. Statistically significant shift by BzATP of the control plot of cumulative probability against the inter-event interval (*Cb*, inset). Change of the absolute amplitude (*Da*) and frequency (*Db*) of the sEPSCs before, 8–10 min after the application of BzATP, and a further 8–10 min of washout. Mean \pm S.E.M. of seven experiments. # $P<0.05$; statistically significant difference from the control value

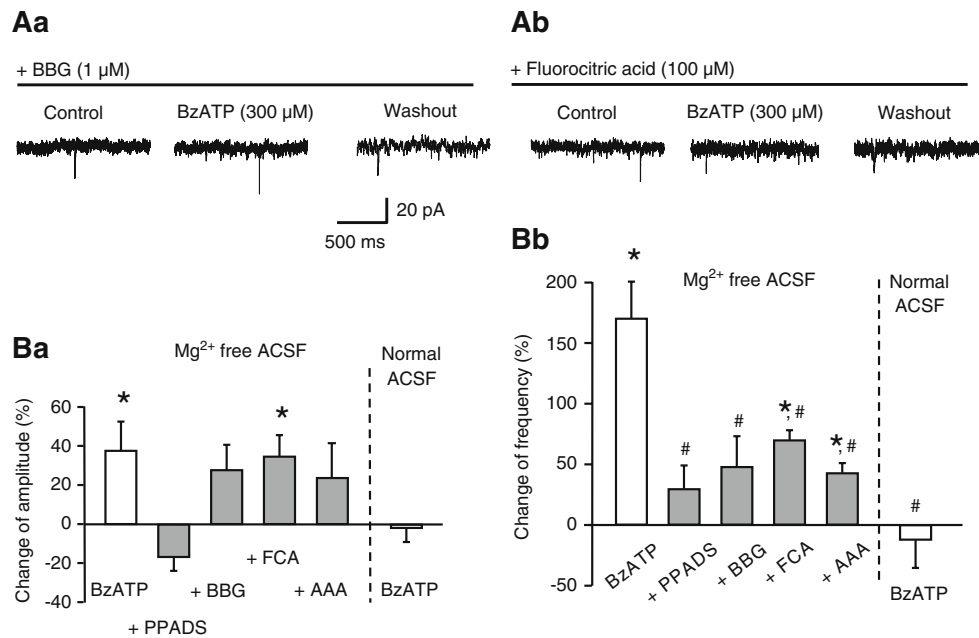


Fig. 6 Blockade by P2 receptor antagonists, selective astrocytic poisons, and external Mg²⁺ of the BzATP-induced change in frequency of sEPSCs in rat LC neurons. Representative recordings of sEPSCs and antagonism by BBG (1 μ M; *Aa*) and fluorocitric acid (100 μ M; *Ab*) of the effect of BzATP (300 μ M). Percentage BzATP-induced changes of the amplitude (*Ba*) and frequency (*Bb*) of sEPSCs in the presence of PPADS (30 μ M) or Brilliant Blue G (BBG; 1 μ M), or their absence, 8–10 min after starting agonist application. Some brain slices were incubated for 2 h in a fluorocitric acid (FCA;

100 μ M)- or amino adipic acid (AAA; 100 μ M)-containing medium, before starting superfusion in the recording chamber; control measurements of the BzATP effect were made on brain slices incubated for a comparable time in drug-free ACSF. The BzATP-induced change in amplitude and frequency in a normal Mg²⁺-containing superfusion medium is shown as the last in each series of columns. Mean \pm S.E.M. of five to six experiments. * P <0.05; statistically significant differences from zero. # P <0.05; statistically significant differences from the effect of BzATP alone

because a 2-h pre-incubation with fluorocitric acid (100 μ M) or amino adipic acid (100 μ M), two selective metabolic poisons of astrocytes, counteracted the effect of BzATP, P2X7 receptors may be located at astrocytes rather than at the LC neurons themselves (Fig. 6*Ab*,*Ba*,*b*).

In further experiments, TTX (0.5 μ M) was added to abolish synaptic transmission and consequently to ensure the recording of monoquantal excitatory events (mEPSCs; Fig. 7). Under these conditions, the facilitation of the mEPSC frequency by BzATP was much less pronounced than that of the sEPSCs (Figs. 5*Db* and 7*Cb*). The BzATP effect became evident as a small rightward shift of the inter-event interval distribution and a comparable leftward displacement of the cumulative probability/inter-event interval plot (Fig. 7*Bb* and its inset). Although the amplitude of mEPSCs also showed a tendency to increase in the presence of BzATP, this change did not reach statistical significance (Fig. 7*Ba*,*Ca*). Thus, BzATP facilitated both the action potential-induced release of glutamate and to a minor degree also the secretion of Ca²⁺ from intracellular stores of the axon terminals or alleviating the release machinery.

The conclusion that the effects of the three P2 agonists investigated are due primarily to a presynaptic effect at glutamatergic afferent fibres terminating at the LC is based

on the observation that 2-MeSATP, ATP and BzATP, all unequivocally increased the sEPSC and/or mEPSC frequency; at the same time, the enhancement of the sEPSC and/or mEPSC amplitude either did not reach (2-MeSATP, ATP) or just surmounted (BzATP) the level of statistical significance and was thereby quite moderate.

Effect of capsaicin and interaction with TRPV1 but not P2X receptor antagonists

The TRPV1 agonist capsaicin has earlier been shown to increase the mEPSC frequency in LC neurons under in situ conditions [21]. We found that, in contrast to 2-MeSATP and ATP, but in accordance with BzATP, capsaicin (10 μ M) did not induce an inward current response of LC neurons ($n=6$; Fig. 8*Aa*). Again in accordance with BzATP, capsaicin failed to increase the sEPSC amplitude in a statistically significant manner (Fig. 8*Ba*), but clearly facilitated the frequency of sEPSCs (Fig. 8*Aa*,*Bb*). Moreover, the selective TRPV1 antagonist capsazepine (30 μ M) abolished the effect of capsaicin, whereas PPADS (30 μ M) had no activity. Thus, TRPV1 and P2X7 receptor agonists both appear to presynaptically facilitate the ongoing glutamatergic input to LC neurons. However, the two transmitter systems are independent of each other, or in

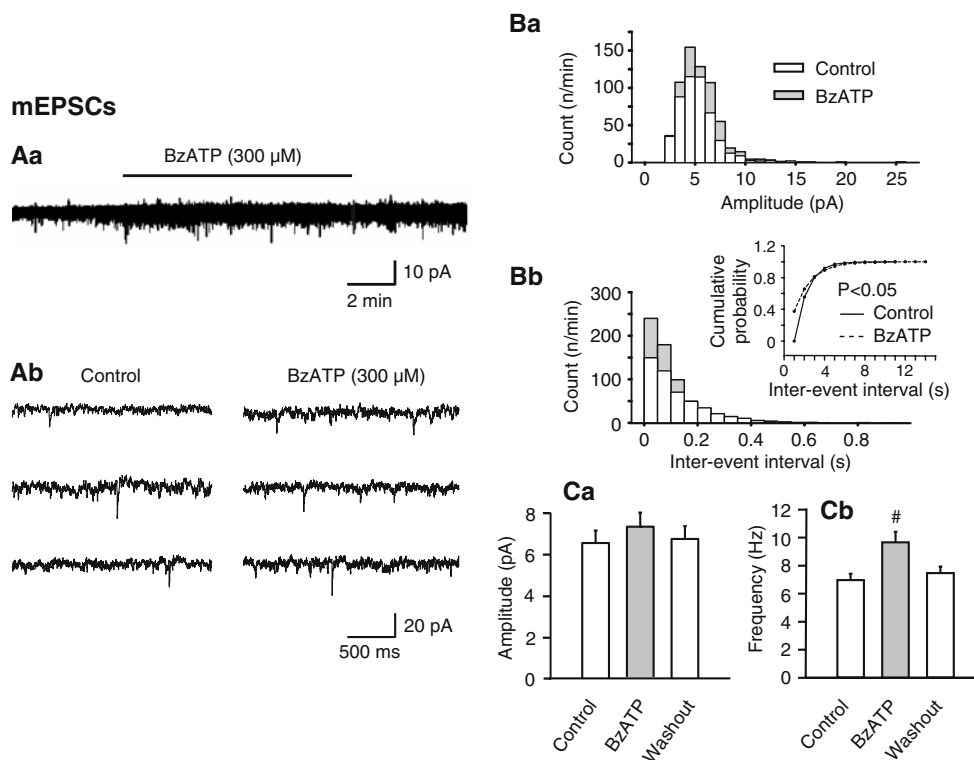


Fig. 7 Effects of BzATP on the amplitude and frequency of mEPSCs in rat LC neurons. mEPSCs were measured in the continuous presence of tetrodotoxin (0.5 μ M). *Aa* Representative recordings of sEPSCs before (*Ab*, left panel) and 8–10 min after (*Ab*, right panel) starting superfusion with BzATP (300 μ M). Note the different time-scales of recording in *Aa* and *Ab* as well as the stability of the holding current in spite of the application of BzATP in *Aa*. *B* Plot of the number of events against the amplitude (*Ba*) and inter-event intervals (*Bb*) in the cell shown in *Aa*

other words, TRPV1 activation does not operate via a purinergic intermediate step.

Discussion

The main finding of this study is that the stimulation of P2X7 receptors leads to an increased release of glutamate onto LC neurons. Although a slight potentiation of the sEPSC amplitude (a measure of postsynaptic sensitivity) occurred in some of the experiments, the facilitation of the sEPSC frequency (a measure of spontaneous transmitter release) was a much more pronounced phenomenon.

The enhancement of spontaneous glutamatergic transmission by ATP has been reported originally for the nociceptive afferent pathways to lamina V [22] and I [23] in the spinal cord dorsal horn. In this case, the general P2 receptor agonist ATP and the P2X1,3 selective agonist α,β -meATP had comparable activities, indicating the involvement of pain-relevant, presynaptic P2X3 receptors [24]. Later on, an ATP-induced facilitation of the sEPSC frequency was demonstrated also for glutamatergically

innervated autonomic nuclei in the medulla oblongata [25–27]. In these experiments, the omission of Ca^{2+} from the bath solution blocked the action of ATP, whereas the pharmacological inhibition of voltage-gated Ca^{2+} channels (VGCCs) was ineffective. Thus, the entry of Ca^{2+} via the P2X receptor-channel complex itself was suggested to occur, rather than the passage of Ca^{2+} through VGCCs opened by the P2X receptor-induced depolarization. Moreover, the role of P2Y receptors, whose effect is known to be independent of extracellular Ca^{2+} was excluded by these experiments. In some, but not all cases, P2X3 receptors appeared to mediate the ATP effect, since α,β -meATP mimicked and preferential P2X3 receptor antagonists such as TNP-ATP [26] or A-317491 [27] antagonised it.

Although P2X receptors presynaptically facilitate the spontaneous excitatory input to the spinal cord and to mesencephalic/pontine nuclei, comparable effects were described also for inhibitory inputs measured as spontaneous inhibitory postsynaptic potentials (sIPSCs). The frequency of GABAergic and glycinergic sIPSCs was reported to be facilitated by P2X receptor activation at the level of the spinal cord [28, 29], mesencephalon [30] and cerebral cortex

and *Ab*. Statistically significant shift by BzATP of the control plot of cumulative probability against the inter-event interval (*Bb*, inset). Change of the absolute amplitude (*Ca*) and frequency (*Cb*) of the mEPSCs before, 8–10 min after starting the application of BzATP, and a further 8–10-min of washout. Mean \pm S.E.M. of five experiments. The time-period elapsing from the beginning of superfusion with BzATP was as in *Aa* and *Ab*. # $P < 0.05$; statistically significant difference from the control value

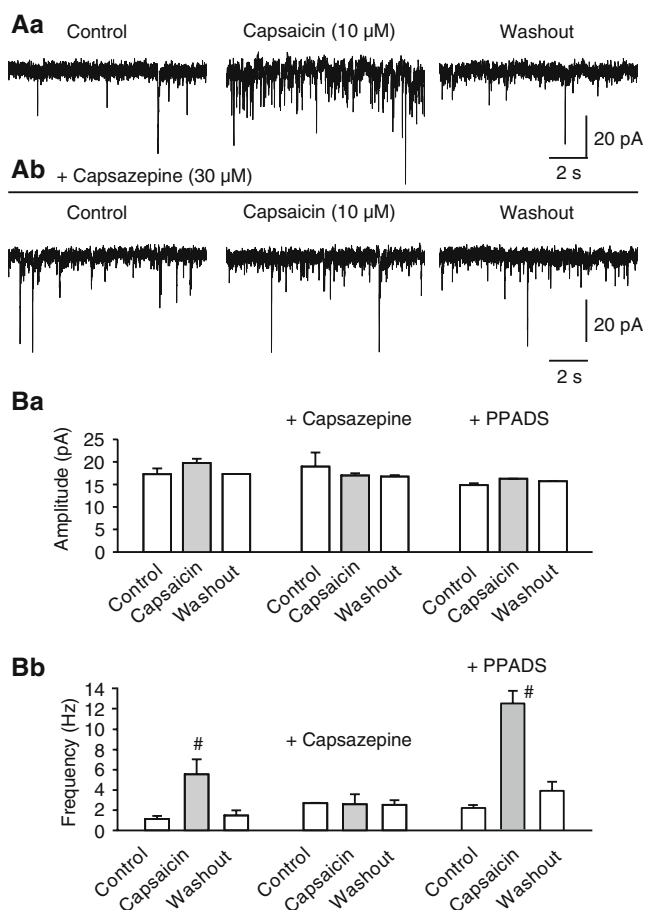


Fig. 8 Effects of capsaicin on the amplitude and frequency of sEPSCs in rat LC neurons; interaction with capsazepine and PPADS. *Aa* Representative recordings of sEPSCs before, and 8–10 min after starting superfusion with capsaicin (10 μM), as well as after a further 8–10 min of washout. *Ab* Representative recordings of sEPSCs before, and 8–10 min after starting superfusion with capsaicin (10 μM), as well as after a further 8–10 min of washout, in the continuous presence of capsazepine (30 μM). Change of the absolute amplitude (*Ba*) and frequency (*Bb*) of the sEPSCs before, during and after the application of capsaicin, in the absence or presence of capsazepine or PPADS (30 μM). Mean ± S.E.M. of six to eight experiments. [#] $P < 0.05$; statistically significant difference from the control value

[31]. The mechanisms of the sEPSC and sIPSC increases were identical in that the presynaptic facilitation was due to the considerable Ca^{2+} permeability of the P2X receptors involved.

We found that the mixed P2X/P2Y receptor agonists, 2-MeSATP and ATP were able to increase the glutamatergic sEPSC frequency in rat LC neurons. The P2X_{1,3} receptor agonistic α, β -meATP and the P2Y_{2,4} receptor agonistic UTP were inactive. These findings in conjunction with the strong facilitatory effect of BzATP are already compatible with the participation of P2X₇ receptors [20, 32]. Although BzATP is known to stimulate all homomeric P2X receptor-types except P2X₅ and P2X₆ at the concentration (300 μM) used, further support for the activation of P2X₇ receptors is

supplied by (1) the more marked effect of BzATP in comparison with that of ATP itself, (2) the failure of BzATP to act in a Mg^{2+} -containing superfusion medium, and (3) the antagonistic effects of PPADS and Brilliant Blue G, but not suramin and reactive blue 2 [12, 13]. Although in the meantime, more selective P2X₇ receptor antagonists were discovered (e.g. A-740003 or A-438079; [20]), Brilliant Blue G is still the prototypic antagonist, which blocks P2X₇ receptors at a 10–100-times higher potency than any other receptor of the P2X family [19].

In contrast to BzATP, 2-MeSATP induced an early inward current, sensitive to PPADS, but not suramin. Moreover, the comparable inward current caused by ATP was blocked by both antagonists. All these results, as well as the inability of suramin to prevent the 2-MeSATP-induced facilitation of the sEPSC frequency suggest, that the postsynaptic P2X receptors at LC neurons may be pharmacologically different from their counterparts regulating the release of glutamate from afferent fibres terminating at the LC. This postsynaptic receptor is certainly not P2X₄, which shares its sensitivity to extracellular Mg^{2+} with P2X₇ [33], but is unaffected by PPADS up to a concentration of 500 μM [20].

It is concluded that the presynaptic effects are mediated by P2X₇ receptors (sensitive to ATP, 2-MeSATP, BzATP, PPADS and Brilliant Blue G, but not α, β -meATP or suramin), whereas the postsynaptic effects are mediated by a hitherto unidentified P2X receptor with unusual properties (sensitive to ATP, 2-MeSATP, suramin and PPADS, but not α, β -meATP and BzATP) [see also 34, 35]. The failure of α, β -meATP to initiate an inward current in spite of producing depolarization and consequently an increased spike discharge [3, 34], may be due to its reported ability to decrease a resting Ca^{2+} -dependent potassium conductance [3].

ATP is an important bidirectional signalling molecule in the brain subserving neuron–astrocyte interactions [36, 37]. This nucleotide may be released from nerve terminals/glia cells by exocytotic mechanisms [37], or only from astrocytic cells via connexin hemichannels, volume-regulated anion channels, ATP-binding cassette transporters and the cystic fibrosis transmembrane regulator [38]. Functional P2X₇ receptors have been identified both at cultured astrocytes [39–42] and astrocytes situated in brain slices [43]. By contrast, enhanced green fluorescent protein-expressing astrocytes acutely dissociated from the cortex of transgenic (Tg(GFAP/EGFP) mice exhibited ATP-induced currents which were mediated by P2X_{1/5} heteromeric, but not P2X₇ homomeric receptors [44]. However, in this case, a complicating factor may be the reported ability of P2X₇ receptors to interact with several cytoskeletal proteins including actin [12, 45]. Actin filament disintegration, such as that occurring during the mechanical dissociation, may

influence the activity of these receptors, potentially by impeding their assembly from monomers into the operative trimeric configuration [46].

The stimulation of astrocytic P2X₇ receptors may lead to the release of glutamate [39], ATP [40], endocannabinoids [47], and interleukin 1- β [41, 48]. Because of the involvement of P2X₇ receptors in inflammation, further inflammatory mediators including prostaglandins and leukotrienes may also be produced and subsequently released into the extracellular space [49]. In the present experiments, we found that the selective astrocytic poisons fluorocitric acid [50] and aminoadipic acid [51], most probably by interfering with the outflow of one or more than one signalling molecules, markedly depressed the BzATP-induced facilitation of sEPSCs. Both fluorocitric acid and aminoadipic acid were used at a concentration (100 μ M) which was reported to interfere with the synthesis, storage and release of amino acid gliotransmitters [52, 53]. Thus, we suggest that P2X₇ receptors are situated at neighbouring astrocytes rather than at the nerve terminals of glutamatergic afferents innervating the LC.

Eventually, we confirmed the findings of Marinelli et al. [21] in that capsaicin facilitated the sEPSC frequency in the LC. In addition, we showed that this effect was prevented by the selective TRPV1 antagonist capsazepine, but not by the P2 receptor antagonist PPADS. Thus, the two algogenic compounds appear to utilise separate receptor systems to potentiate the release of glutamate, although the resulting excitability increase of LC neurons, most likely involved in pain sensation, is identical.

Acknowledgements We are grateful to Dr. Thomas Riedel for many helpful discussions. Fellowships from the Tarbiat Modares University, Teheran, Iran and the DAAD/MÖB (332 4 00 138/PPP) financed the stays of Mrs. Roghayeh Khakhpay and Dr. Laszlo Köles in Leipzig, respectively. This work was supported by grants from the Deutsche Forschungsgemeinschaft (IL 20/16-1; IL 20/19-1) and the Volkswagen Foundation (I/82 940).

References

1. Stamford JA (1995) Descending control of pain. *Br J Anaesth* 75:217–227
2. Van Bockstaele EJ, Aston-Jones G (1995) Integration in the ventral medulla and coordination of sympathetic, pain and arousal functions. *Clin Exp Hypertens* 17:153–165
3. Harms L, Finta EP, Tschöpl M, Illes P (1992) Depolarization of rat locus coeruleus neurons by adenosine 5'-triphosphate. *Neuroscience* 48:941–952
4. Shen KZ, North RA (1993) Excitation of rat locus coeruleus neurons by adenosine 5'-triphosphate: ionic mechanism and receptor characterization. *J Neurosci* 13:894–899
5. Aghajanian GK, Wang YY (1987) Common alpha 2- and opiate effector mechanisms in the locus coeruleus: intracellular studies in brain slices. *Neuropharmacology* 26:793–799
6. Cherubini E, North RA, Williams JT (1988) Synaptic potentials in rat locus coeruleus neurones. *J Physiol* 406:431–442
7. Williams JT, Bobker DH, Harris GC (1991) Synaptic potentials in locus coeruleus neurons in brain slices. *Prog Brain Res* 88:167–172
8. Egan TM, Henderson G, North RA, Williams JT (1983) Noradrenaline-mediated synaptic inhibition in rat locus coeruleus neurones. *J Physiol* 345:477–488
9. Nieber K, Poelchen W, Illes P (1997) Role of ATP in fast excitatory synaptic potentials in locus coeruleus neurones of the rat. *Br J Pharmacol* 122:423–430
10. Poelchen W, Sieler D, Wirkner K, Illes P (2001) Co-transmitter function of ATP in central catecholaminergic neurons of the rat. *Neuroscience* 102:593–602
11. Virginio C, MacKenzie A, Rassendren FA, North RA, Surprenant A (1999) Pore dilation of neuronal P2X receptor channels. *Nat Neurosci* 2:315–321
12. Sperlágh B, Vizi ES, Wirkner K, Illes P (2006) P2X₇ receptors in the nervous system. *Prog Neurobiol* 78:327–346
13. Anderson CM, Nedergaard M (2006) Emerging challenges of assigning P2X₇ receptor function and immunoreactivity in neurons. *Trends Neurosci* 29:257–262
14. Di Virgilio F (2007) Liaisons dangereuses: P2X₇ and the inflammasome. *Trends Pharmacol Sci* 28:465–472
15. Hughes JP, Hatcher JP, Chessell IP (2007) The role of P2X₇ in pain and inflammation. *Purinergic Signal* 3:163–169
16. Minke B, Cook B (2002) TRP channel proteins and signal transduction. *Physiol Rev* 82:429–472
17. Wirkner K, Franke H, Inoue K, Illes P (1998) Differential age-dependent expression of α_2 adrenoceptor- and P2 purinoceptor-functions in rat locus coeruleus neurons. *Naunyn Schmiedeberg Arch Pharmacol* 357:186–189
18. Barry PH (1994) JPCalc, a software package for calculating liquid junction potential corrections in patch-clamp, intracellular, epithelial and bilayer measurements and for correcting junction potential measurements. *J Neurosci Methods* 51:107–116
19. Khakh BS, Burnstock G, Kennedy C, King BF, North RA, Séguéla P, Voigt M, Humphrey PP (2001) International Union of Pharmacology. XXIV. Current status of the nomenclature and properties of P2X receptors and their subunits. *Pharmacol Rev* 53:107–118
20. Jarvis MF, Khakh BS (2009) ATP-gated P2X cation-channels. *Neuropharmacology* 56:208–215
21. Marinelli S, Vaughan CW, Christie MJ, Connor M (2002) Capsaicin activation of glutamatergic synaptic transmission in the rat locus coeruleus in vitro. *J Physiol* 543:531–540
22. Nakatsuka T, Gu JG (2001) ATP P2X receptor-mediated enhancement of glutamate release and evoked EPSCs in dorsal horn neurons of the rat spinal cord. *J Neurosci* 21:6522–6531
23. Chen M, Gu JG (2005) A P2X receptor-mediated nociceptive afferent pathway to lamina I of the spinal cord. *Mol Pain* 1:1–13
24. Chizh BA, Illes P (2001) P2X receptors and nociception. *Pharmacol Rev* 53:553–568
25. Khakh BS, Henderson G (1998) ATP receptor-mediated enhancement of fast excitatory neurotransmitter release in the brain. *Mol Pharmacol* 54:372–378
26. Shigetomi E, Kato F (2004) Action potential-independent release of glutamate by Ca²⁺ entry through presynaptic P2X receptors elicits postsynaptic firing in the brainstem autonomic network. *J Neurosci* 24:3125–3135
27. Watano T, Calvert JA, Vial C, Forsythe ID, Evans RJ (2004) P2X receptor subtype-specific modulation of excitatory and inhibitory synaptic inputs in the rat brainstem. *J Physiol* 558:745–757
28. Hugel S, Schlichter R (2000) Presynaptic P2X receptors facilitate inhibitory GABAergic transmission between cultured rat spinal cord dorsal horn neurons. *J Neurosci* 20:2121–2130

29. Rhee JS, Wang ZM, Nabekura J, Inoue K, Akaike N (2000) ATP facilitates spontaneous glycinergic IPSC frequency at dissociated rat dorsal horn interneuron synapses. *J Physiol* 524:471–483
30. Jameson HS, Pinol RA, Mendelowitz D (2008) Purinergic P2X receptors facilitate inhibitory GABAergic and glycinergic neurotransmission to cardiac vagal neurons in the nucleus ambiguus. *Brain Res* 1224:53–62
31. Wirkner K, Köfalvi A, Fischer W, Günther A, Franke H, Gröger-Arndt H, Nörenberg W, Madarász E, Vizi ES, Schneider D, Sperlágh B, Illes P (2005) Supersensitivity of P2X receptors in cerebrocortical cell cultures after in vitro ischemia. *J Neurochem* 95:1421–1437
32. von Kügelgen I (2006) Pharmacological profiles of cloned mammalian P2Y-receptor subtypes. *Pharmacol Ther* 110:415–432
33. Negulyaev YA, Markwardt F (2000) Block by extracellular Mg^{2+} of single human purinergic P2X₄ receptor channels expressed in human embryonic kidney cells. *Neurosci Lett* 279:165–168
34. Tschöpl M, Harms L, Nörenberg W, Illes P (1992) Excitatory effects of adenosine 5'-triphosphate on rat locus coeruleus neurons. *Eur J Pharmacol* 213:71–77
35. Fröhlich R, Boehm S, Illes P (1996) Pharmacological characterization of P2 purinoceptor types in rat locus coeruleus neurons. *Eur J Pharmacol* 315:255–261
36. Fields RD, Burnstock G (2006) Purinergic signalling in neuron–glia interactions. *Nat Rev Neurosci* 7:423–436
37. Burnstock G (2006) Historical review: ATP as a neurotransmitter. *Trends Pharmacol Sci* 27:166–176
38. Illes P, Ribeiro AJ (2004) Molecular physiology of P2 receptors in the central nervous system. *Eur J Pharmacol* 483:5–17
39. Duan S, Anderson CM, Keung EC, Chen Y, Chen Y, Swanson RA (2003) P2X₇ receptor-mediated release of excitatory amino acids from astrocytes. *J Neurosci* 23:1320–1328
40. Suadicani SO, Brosnan CF, Scemes E (2006) P2X₇ receptors mediate ATP release and amplification of astrocytic intercellular Ca^{2+} signaling. *J Neurosci* 26:1378–1385
41. Abbracchio MP, Ceruti S (2006) Roles of P2 receptors in glial cells: focus on astrocytes. *Purinergic Signal* 2:595–604
42. Carrasquero LM, Delicado EG, Bustillo D, Gutiérrez-Martín Y, Artalejo AR, Miras-Portugal MT (2009) P2X₇ and P2Y₁₃ purinergic receptors mediate intracellular calcium responses to BzATP in rat cerebellar astrocytes. *J Neurochem* 110:879–889
43. Fellin T, Pozzan T, Carmignoto G (2006) Purinergic receptors mediate two distinct glutamate release pathways in hippocampal astrocytes. *J Biol Chem* 281:4274–4284
44. Lalo U, Pankratov Y, Wichert SP, Rossner MJ, North RA, Kirchhoff F, Verkhratsky A (2008) P2X₁ and P2X₅ subunits form the functional P2X receptor in mouse cortical astrocytes. *J Neurosci* 28:5473–5480
45. Surprenant A, North RA (2009) Signaling at purinergic P2X receptors. *Annu Rev Physiol* 71:333–359
46. Li Q, Luo X, Zeng W, Muallem S (2003) Cell-specific behavior of P2X₇ receptors in mouse parotid acinar and duct cells. *J Biol Chem* 278:47554–47561
47. Witting A, Walter L, Wacker J, Möller T, Stella N (2004) P2X₇ receptors control 2-arachidonoylglycerol production by microglial cells. *Proc Natl Acad Sci USA* 101:3214–3219
48. Ferrari D, Pizzirani C, Adinolfi E, Lemoli RM, Curti A, Idzko M, Panther E, Di Virgilio F (2006) The P2X₇ receptor: a key player in IL-1 processing and release. *J Immunol* 176:3877–3883
49. Qu Y, Franchi L, Nunez G, Dubyak GR (2007) Nonclassical IL-1 beta secretion stimulated by P2X₇ receptors is dependent on inflammasome activation and correlated with exosome release in murine macrophages. *J Immunol* 179:1913–1925
50. Clarke DD (1991) Fluoroacetate and fluorocitrate: mechanism of action. *Neurochem Res* 16:1055–1058
51. Huck S, Grass F, Hörtnagl H (1984) The glutamate analogue alpha-amino adipic acid is taken up by astrocytes before exerting its gliotoxic effect in vitro. *J Neurosci* 4:2650–2657
52. Deleuze C, Duvoid A, Hussy N (1998) Properties and glial origin of osmotic-dependent release of taurine from the rat supraoptic nucleus. *J Physiol* 507:463–471
53. McBean GJ (1994) Inhibition of the glutamate transporter and glial enzymes in rat striatum by the gliotoxin, α -amino adipate. *Br J Pharmacol* 113:536–540